ADAPTIVE BAYESIAN TRACKING WITH UNKNOWN TIME-VARYING SENSOR NETWORK PERFORMANCE

Giuseppe Papa[⋆], *Paolo Braca*[⋆], *Steven Horn*[⋆], *Stefano Marano*[‡], *Vincenzo Matta*[‡] *and Peter Willett*[†]

[⋆] NATO STO CMRE, La Spezia, Italy, Email: {giuseppe.papa/paolo.braca/steven.horn}@cmre.nato.int.
[‡] University of Salerno, Fisciano, Italy, Email: {marano/vmatta}@unisa.it.
[†] University of Connecticut, Storrs CT, Email: willett@engr.uconn.edu.

ABSTRACT

In practical target tracking problems, the target detection performance of the sensors may be unknown and may change rapidly with time. In this work we develop a target tracking procedure able to adapt and react to time-varying changes of the detection capability for a network of sensors. The proposed tracking strategy is based on a Bayesian framework, in which the dynamic target state is augmented to include the sensor detection probabilities. The method is validated using computer simulations and real-world experiments conducted by the NATO Science and Technology Organization (STO) - Centre for Maritime Research and Experimentation (CMRE).

Index Terms— Multiple sensors, real-world data, Bayesian target tracking, particle filter, time-varying performance.

1. MOTIVATION AND RELATED WORK

Multi-sensor target tracking is a challenging problem which involves data fusion of measurements from multiple sensors to perform joint detection and estimation of a moving object [1]. Measurements are usually subject to noise, missed detections, and false alarms. To cope with such non-idealities in the sensor model, the majority of target tracking algorithms assume the parameters which describe the statistical behaviour of the collected returns are known. However, in real-world applications these parameters may exhibit marked spatio-temporal variations, and this will have a strong effect on the capability of the tracking algorithms.

A typical scenario is that of manoeuvring targets in which the behaviour of a target cannot be characterized at all times by a single dynamic model and a solution should estimate on-line the proper dynamics assumed to model the target at the current time. The usual mechanism for this is often the interacting multiple model (IMM), see *e.g.* [2]. In several practical applications, a similar phenomenon can be observed for the performance of the sensors themselves, as opposed to the target dynamics. Now, in filtering problems the task of detecting – and sequestering – faulty sensors has been studied, see *e.g.* [3]; however, in target tracking problems, even if the sensor is working correctly, its capability of observing a target can be affected by several factors, often difficult to characterize and model properly. Consider, for example, the degradation of detection capability when the target aspect is not favourable in terms of geometry with respect to the sensor, or when the signal-to-noise ratio (SNR) is completely unknown, see *e.g.* [4]. Another example is interference in backscattered power due to the Bragg effect in HF surface wave radars [5]. In underwater sonar systems, target detections are influenced by several environmental effects – for instance sound propagation – which have a strong dependence on unknown parameters (*e.g.* temperature, salinity, etc.) [6] that may change rapidly in time [7].

While a broad part of target tracking literature considers the sensor performance to be a given, *e.g.* see [8, 9, 10, 11, 12, 13, 14, 15, 16, 17, 18], and consequently the algorithm parameters perfectly matched to truth, only few recent papers focus on the problem of a mismatch of the sensor parameters, see [7, 4, 19, 20, 21].

The key aspect of this work is that the sensor detection capability of a target is not only unknown and spatially dependent, but that it may change rapidly in time. A target tracking procedure will be developed to adapt to the changes in the sensor detection capability. In particular, a full Bayesian framework is derived to model the behaviour of a network of sensors in which each sensor has its own time-varying detection capability. The dynamic target state is augmented to add the detection probabilities of each sensor in the network, and the dynamics of this detection probability are modeled as a time-varying Markov process.

This proposed method is validated using both computer experiments and real-world data collected during the CMRE HF-radar experiment, which took place between May and December 2009 on the Ligurian coast of the Mediterranean Sea, see more details in [5].

2. PROBLEM FORMALIZATION

Consider a system consisting of a network of N_s sensors, whose aim is to monitor a surveillance region. In particular, the aim is to detect target presence/absence and, in the case of presence, to track the target state. Without loss of generality we consider a two-dimensional surveillance region with area V. At time scan k the target of interest can be present or absent. When the target is present, its state is $\boldsymbol{x}_k = [p_k^x, \dot{p}_k^x, p_k^y, \dot{p}_k^y]^T$, where p_k^x and p_k^y are the position coordinates and $\dot{p}_k^x$ and $\dot{p}_k^y$ are the velocities in the two dimensions. For ease of notation, we also define the set X_k, where $X_k = \emptyset$ when the target is absent, otherwise $X_k = \{\boldsymbol{x}_k\}$. This is a compact representation of the target presence/absence and the target state. In the target tracking literature, see *e.g.* [22], X_k is often referred to as a Bernoulli Random Finite Set (RFS) [9, 12, 15, 16, 17]. The time evolution of X_k is ruled by the distribution

$$\phi_X\left(X_k|X_{k-1}\right) = \begin{cases} 1-p_b, & X_k=\emptyset, X_{k-1}=\emptyset, \\ p_b\ f_b\left(\boldsymbol{x}_k\right), & X_k=\left\{\boldsymbol{x}_k\right\}, X_{k-1}=\emptyset, \\ 1-p_s, & X_k=\emptyset, X_{k-1}=\left\{\boldsymbol{x}_{k-1}\right\}, \\ p_s\ f\left(\boldsymbol{x}_k|\boldsymbol{x}_{k-1}\right), & X_k=\left\{\boldsymbol{x}_k\right\}, X_{k-1}=\left\{\boldsymbol{x}_{k-1}\right\}, \end{cases} \quad (1)$$

where p_b and $f_b(\boldsymbol{x})$ are respectively the target *birth* probability and the target birth distribution, while p_s and $f(\boldsymbol{x}_k|\boldsymbol{x}_{k-1})$ are respectively the target *survival* probability and the target state transition distribution. The latter is often given by the relation $\boldsymbol{x}_k = \boldsymbol{F}_k(\boldsymbol{x}_{k-1}, \boldsymbol{v}_k)$, where $\boldsymbol{F}_k$ is the state transition function (in general non-linear) and $\boldsymbol{v}_k$ is the process noise, often assumed as a sequence of independent and identically distributed (i.i.d.) random variables.

2.1. Measurement origin uncertainty

This section describes the measurement origin uncertainty (MOU) model, widely used in the tracking literature to describe missed target detections and clutter [1].

At time scan k a sensor $s = 1, 2, \ldots, N_s$ can detect a target with a probability of detection, denoted by p_k^s. This probability is modeled in the proposed approach as time dependent. Furthermore, spurious measurements (clutter), not originating from, and independent from the target, are also observed. The set of measurements from sensor s at time scan k is defined as

$$Z_k^s = \left\{\boldsymbol{z}_{k,i}^s, i = 1, 2, \ldots, m_k^s\right\}, \tag{2}$$

where m_k^s is the total number of measurements from sensor s at time scan k.

If the target is present at time scan k, then the target-originated measurement of the sensor s is given by

$$\boldsymbol{z}_k^s = \boldsymbol{h}_s(\boldsymbol{x}_k, \boldsymbol{w}_k^s), \tag{3}$$

where $\boldsymbol{h}_s$ is the measurement function and $\boldsymbol{w}_k^s$ is an i.i.d. measurement noise sequence. If the target is detected by the sensor, then $\boldsymbol{z}_k^s \in Z_k^s$.

Since the sensors are conditionally independent given the target state, the likelihood of the measurements is [18]

$$\mathcal{P}(Z_k|X_k, \boldsymbol{p}_k) = \prod_{s=1}^{N_s} \mathcal{P}(Z_k^s|X_k, p_k^s), \tag{4}$$

where $Z_k \stackrel{def}{=} \left\{Z_k^1, \ldots, Z_k^{N_s}\right\}$ and $\boldsymbol{p}_k \stackrel{def}{=} \left[p_k^1, \ldots, p_k^{N_s}\right]^T$. The likelihood for the sensor s, when the target is absent, is given only by clutter data

$$\mathcal{P}(Z_k^s|\emptyset, p_k^s) = \mathcal{P}(Z_k^s|\emptyset) = \phi_C^s(Z_k^s), \tag{5}$$

$$\phi_C^s(Z_k^s) = \begin{cases} m_k^s!\mu(m_k^s; \lambda^s) \prod_{\boldsymbol{z}\in Z_k^s} c^s(z), & m_k^s > 0, \\ \mu(0; \lambda^s), & m_k^s = 0, \end{cases}$$

where $\mu(m; \lambda^s)$ and λ^s are respectively the distribution and the average number of clutter elements, while $c^s(\boldsymbol{z})$ is the PDF of a clutter element. Often, $\mu(m; \lambda^s)$ is assumed to be Poisson and $c^s(z)$ uniform [18, 6].

It is possible to show that the likelihood for the sensor s, when the target is present, is given by

$$\mathcal{P}(Z_k^s|\{\boldsymbol{x}_k\}, p_k^s) = (1 - p_k^s)\,\phi_C^s(Z_k^s) + \\ + p_k^s \sum_{\boldsymbol{z}\in Z_k^s} f(\boldsymbol{z}|\boldsymbol{x}_k)\,\phi_C^s(Z_k^s \backslash \boldsymbol{z}) \tag{6}$$

It is worth noting that when $p_k^s = 0$ (target present but not observable), the likelihoods (5) and (6) coincide and it is not possible to distinguish statistically between the case of target presence and absence[1]. Consequently, it is assumed that p_k^s cannot have values below a given threshold $p_{min}^s > 0$.

Algorithm 1 Adaptive Tracker using particle filtering.

IMPORTANCE SAMPLING
`Draw` $\boldsymbol{x}_k^i \sim f\left(\boldsymbol{x}_k|\boldsymbol{x}_{k-1}^i\right), \quad \forall i = 1, \ldots, N_p;$
`Draw` $\boldsymbol{p}_k^i \sim f_p\left(\boldsymbol{p}_k|\boldsymbol{p}_{k-1}^i\right), \quad \forall i = 1, \ldots, N_p;$
for $s = 1$ **to** N **do**
  `Draw` N_n `new samples` $\boldsymbol{x}_k^i$ `from` $\mathcal{U}\left(\boldsymbol{x}; \boldsymbol{z}_{k,i}^s\right)$
  `and` $\boldsymbol{p}_k^i$ `from` $\mathcal{U}(\boldsymbol{p}), \quad \forall i = 1, \ldots, |Z_k^s|;$
end for

UPDATE
for $i = 1$ **to** $N_p + N_n N_{Z_k}$ **do**
  $X_k^i = \left\{\left(\boldsymbol{x}_k^i, \boldsymbol{p}_k^i\right)\right\}, \quad w_k^i = \mathcal{L}\left(Z_k|X_k^i\right) \frac{\phi_X\left(X_k^i|X_{k-1}^i\right)}{q\left(X_k^i|X_{k-1}^i, Z_k\right)} w_{k-1}^i;$
end for
$w_k^\emptyset = \mathcal{L}(Z_k|X_k = \emptyset)\left[(1 - p_b)\, w_{k-1}^\emptyset + (1 - p_s)\left(1 - w_{k-1}^\emptyset\right)\right];$
`Drop the particles with the lowest` $N_n N_{Z_k}$ `weights;`

NORMALIZATION
$w_t = w_k^\emptyset + \sum_{j=1}^{N_p} w_k^i;$ {Total weight}
$w_k^\emptyset = \frac{w_k^\emptyset}{w_t}; \qquad w_k^i = \frac{w_k^i}{w_t}, \quad \forall i = 1, \ldots, N_p;$

RESAMPLING
$N_{eff} = \left(\sum_{j=1}^{N_p} {w_k^i}^2\right)^{-1};$ {Effective sample size}
if $N_{eff} < N_p T_d$ **then**
  `resampling;`
end if

3. ADAPTIVE TRACKER

In real-world applications, the detection performance of a sensor p_k^s is usually time-varying and spatially-varying, because it depends on environmental conditions, aspect, interference, etc. (see *e.g.* [7, 5, 6]). Now, it is noted that the likelihood (6) is strongly dependent on the sensor detection probabilities, and, consequently, a sequential Bayesian procedure is proposed in which the detection probabilities are included in the dynamic system state. The state at time k is then redefined as $X_k = \{(\boldsymbol{x}_k, \boldsymbol{p}_k)\}$, when the target is present, while it remains $X_k = \emptyset$, when the target it absent. The posterior distribution given all the measurements up to time scan k is given by

$$\mathcal{P}(X_k|Z_{1:k}) = \frac{\mathcal{L}(Z_k|X_k)\,\mathcal{P}(X_k|Z_{1:k-1})}{\mathcal{P}(Z_k|Z_{1:k-1})}, \tag{7}$$

where $Z_{1:k} \stackrel{def}{=} \{Z_1, \ldots, Z_k\}$ and $\mathcal{L}(Z_k|X_k)$ is given by eq. (4)-(5)-(6)

$$\mathcal{L}(Z_k|\emptyset) = \prod_{s=1}^{N_s} \mathcal{P}(Z_k^s|\emptyset), \tag{8}$$

$$\mathcal{L}(Z_k|\{(\boldsymbol{x}_k, \boldsymbol{p}_k)\}) = \prod_{s=1}^{N_s} \mathcal{P}(Z_k^s|\{\boldsymbol{x}_k\}, \boldsymbol{p}_k). \tag{9}$$

[1] This work considers the case of target not present and target not observable to be the same case.

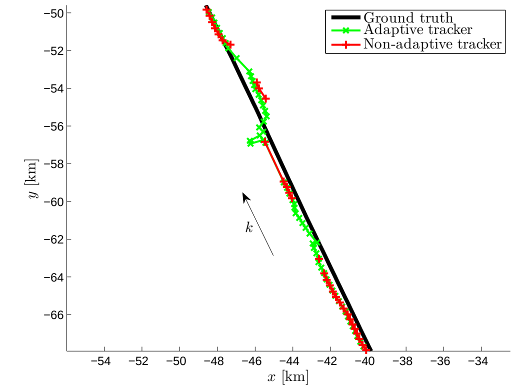

(a) HFSW radar tracks and ground-truth (AIS).

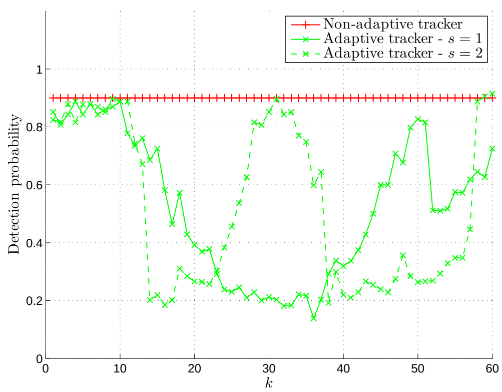

(b) Time-varying detection probability profile.

Fig. 1. Comparison between the adaptive and non-adaptive tracker using the dataset of two HFSW radar systems (WERA). Panel (a) presents the trajectories, when the target is declared as present, and the ground-truth given by the AIS messages. Panel (b) presents the value of the detection probability, constant and fixed to 0.9 for the non-adaptive tracker, while for the adaptive tracker the mode of the posterior distribution of the detection probability for the two sensors, $s = 1, 2$, is shown.

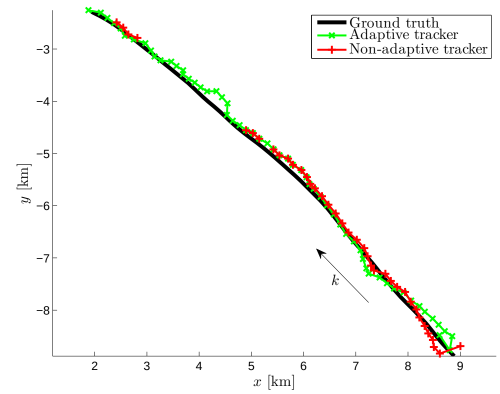

(a) Tracks generated using simulated data.

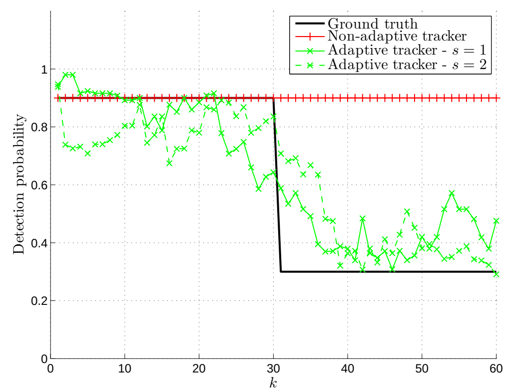

(b) Time-varying detection probability profile.

Fig. 2. Comparison between the adaptive and non-adaptive tracker using simulated data. In panel (a) the trajectories, when the target is declared as present, are reported. Panel (b) presents the value of the detection probability, constant and fixed to 0.9, for the non-adaptive tracker, while for the adaptive tracker we report the mode of the posterior distribution of the detection probability for the two sensors, $s = 1, 2$. An abrupt change in the true detection probability is simulated at the time scan $k = 30$.

The prediction term can be written as

$$\begin{aligned}&\mathcal{P}\left(X_k|Z_{1:k-1}\right) = \phi_X(X_k|\emptyset)\mathcal{P}\left(\emptyset|Z_{1:k-1}\right) + \\ &+ \iint \phi_X\left(X_k|\left\{(\boldsymbol{x},\boldsymbol{p})\right\}\right)\mathcal{P}\left(\left\{(\boldsymbol{x},\boldsymbol{p})\right\}|Z_{1:k-1}\right)d\boldsymbol{x}d\boldsymbol{p},\end{aligned}$$

the RFS transition distribution for the augmented state is indicated with $\phi_X\left(X_k|X_{k-1}\right)$. Note that this distribution has the same structure of eq. (1). There are two functions to be defined: the birth distribution $f_b\left(\boldsymbol{x}_k,\boldsymbol{p}_k\right)$; and the state transition distribution $f_{x,p}\left(\boldsymbol{x}_k,\boldsymbol{p}_k|\boldsymbol{x}_{k-1},\boldsymbol{p}_{k-1}\right)$. This latter can be recast as

$$f_{x,p}\left(\boldsymbol{x}_k,\boldsymbol{p}_k|\boldsymbol{x}_{k-1},\boldsymbol{p}_{k-1}\right) = f\left(\boldsymbol{x}_k|\boldsymbol{x}_{k-1}\right)f_p\left(\boldsymbol{p}_k|\boldsymbol{p}_{k-1},\boldsymbol{x}_k\right),$$

where $f_p\left(\boldsymbol{p}_k|\boldsymbol{p}_{k-1},\boldsymbol{x}_k\right)$ is the detection probability transition distribution, formally dependent from the target state (*e.g.* the geometry target-sensor). Assuming that the sensors are conditionally independent, the detection probability transition distribution is given by

$$f_p(\boldsymbol{p}_k|\boldsymbol{p}_{k-1},\boldsymbol{x}_k) = \prod_{s=1}^{N_s} f_p^s(p_k^s|p_{k-1}^s,\boldsymbol{x}_k), \qquad (10)$$

where each $f_p^s(p_k^s|p_{k-1}^s,\boldsymbol{x}_k)$ is the transition distribution of the corresponding p_k^s of the sensor s.

3.1. Particle filter implementation

Since a closed form for (7) is hard (or even impossible) to derive, a numerical implementation of the filter based on the Sequential Monte Carlo methods [23] applied to RFS [24] is employed. The posterior distribution at time scan k (7) is represented by

$$\hat{\mathcal{P}}\left(X_k|Z_{1:k}\right) = \begin{cases} w_k^{\emptyset}, & X_k = \emptyset, \\ \sum_{i=1}^{N_p} w_k^i \delta_{\boldsymbol{x}_k^i,\boldsymbol{p}_k^i}\left(\boldsymbol{x},\boldsymbol{p}\right), & X_k = \left\{(\boldsymbol{x},\boldsymbol{p})\right\}, \end{cases} \qquad (11)$$

where $w_k^{\emptyset}$ is the weight approximating $\mathcal{P}\left(X_k = \emptyset|Z_{1:k}\right)$, $\left(\boldsymbol{x}_k^i,\boldsymbol{p}_k^i\right)$ is the i-th sample of the augmented system state, w_k^i is the i-th weight approximating $\mathcal{P}\left(X_k = \left\{\left(\boldsymbol{x}_k^i,\boldsymbol{p}_k^i\right)\right\}|Z_{1:k}\right)$, N_p is the number of particles.

Algorithm 1 presents the pseudo-code of the particle filter implementation for the augmented sequential Bayesian filter, referred as the adaptive tracker. Note that the resampling algorithm is standard and given in [23].

The initial samples $\boldsymbol{x}_0^i$ are uniformly drawn in the surveillance area for the positional coordinates and in $[-v_{max}, v_{max}]$ for the speed coordinates, while the initial samples $\boldsymbol{p}_0^i$ are uniformly drawn in $\Omega_1 \times \cdots \times \Omega_{N_s}$, where Ω_s is the support of the detection probability distribution. For instance, assuming a continuous distribution the support is defined as $\Omega_s = [p_{min}^s, 1]$. The initial weights w_0^i are all initialized to $(2N_p)^{-1}$, while $w_0^{\emptyset} = 0.5$. In the importance sampling step of the filter, two kinds of importance sampling distributions are used. The first one is the augmented system state transition distribution and is used to predict the new samples $\left(\boldsymbol{x}_k^i, \boldsymbol{p}_k^i\right)$, $\forall i = 1, \ldots, N_p$, from the N_p samples at the previous step. The second one is constructed on the basis of the measurements Z_k and can be interpreted as the target birth distribution. For each measurement $\boldsymbol{z} \in Z_k^s, \forall s$, N_n particles $\left(\boldsymbol{x}_k^i, \boldsymbol{p}_k^i\right)$ are sampled, where $\boldsymbol{x}_k^i$ is drawn from $\mathcal{U}\left(\boldsymbol{x}; \boldsymbol{z}\right)$, which is the uniform distribution in $[-v_{max}, v_{max}]$ for the speed coordinates and centered in $\boldsymbol{z}$ with a given width for the position coordinates, and $\boldsymbol{p}_k^i$ is drawn from $\mathcal{U}\left(\boldsymbol{p}\right)$, which is a uniform distribution in $\Omega_1 \times \cdots \times \Omega_{N_s}$. The total number of new particles is $N_n N_{Z_k}$, where $N_{Z_k} = \sum_{s=1}^{N_s} |Z_k^s|$.

4. EXPERIMENTAL RESULTS

This section reports the results of the adaptive tracker, using both computer simulated experiments and real-world data collected during the CMRE HF-radar experiment, see details in [5]. Two Wellen radar (WERA) systems were deployed on the Italian coast of the Ligurian Sea, one on Palmaria island near La Spezia (44° 2′ 30″ N, 9° 50′ 36″ E) and the other at San Rossore Park near Pisa (43° 40′ 53″ N, 10° 16′ 52″ E). The target state is defined in Cartesian coordinates, with a fixed origin located at the Palmaria radar site.

Consider the real track of a vessel sailing North-West, as reported by the data transmitted by its Automatic Identification System (AIS) transponder. The AIS track positions, based on GPS, are referred to here as the ground-truth, see also the discussion in [5]. Figure 1(a) reports the tracks generated by the proposed adaptive tracking procedure and the non-adaptive one with fixed detection probabilities for both the sensors. The parameters of the algorithms are reported in Tab. 1. Note that all of the parameters of each of the algorithms are identical, including the number of particles, even though state augmentation should require, in theory, a larger number of particles. The only difference is in the use of the detection probability (fixed for the non-adaptive tracker).

The presence or absence of the target at each frame is decided based on the value of the marginal posterior probability $\mathcal{P}\left(\emptyset | Z_{1:k}\right)$, and if, for instance, this probability exceeds a given threshold then the target absence is declared. In the scenario reported in Figure 1 it is easy to verify that the target trajectory is completely reconstructed by the adaptive tracker while the non-adaptive tracker exhibits some "gaps" in the estimated track. This phenomenon seems to be caused by abrupt decreases of the detection probability in one (or both) of the two radars with respect to the nominal values, these calibrated and fixed to 0.9 for the non-adaptive tracker. Calibrating the values for a non-adaptive tracker is often an ad-hoc process, or possibly as a calibration of static parameters [5]. It is worthwhile to note that the adaptive tracker has the ability to follow these apparent oscillations in detection probability, see Figure 1(b), resulting in better track hold. For the sake of further clarity, this phenomenon is also reconstructed using synthetic data.

Par.	*Simulation*	*HFSW Radar*	*Specification*
T	40 s	33.28 s	Time scan
σ_v	$5\ 10^{-3}\,\mathrm{m/s^2}$	$5\ 10^{-3}\,\mathrm{m/s^2}$	Process noise st. dev.
σ_r	75 m	75 m	Range st. dev.
σ_b	1°	1°	Bearing st. dev.
λ/V	$1.2\,10^{-8}\,\mathrm{m}^{-2}$	$2\,10^{-9}\,\mathrm{m}^{-2}$	Clutter density
N_p	$5\ 10^4$	$5\ 10^4$	Number of particles
p_b	10^{-2}	10^{-4}	Birth probability
p_s	$1-10^{-3}$	$1-10^{-4}$	Survival probability
N_s	2	2	Number of sensors
N_n	250	250	Particles per meas.
T_d	0.5	0.5	Degeneracy threshold

Table 1. Parameter values used in in the algorithm for simulated and real radar data.

Consider the scenario reported in Figure 2, in which the target is sailing North-West. The data are generated using the MOU model, described in Sec. 2.1 and with the parameters reported in Tab. 1, with the true value of the detection probability for both the sensors fixed at 0.9 in first 30 scans followed by an abrupt decrease to 0.3. This simulates such phenomena as unfavorable propagation, interference or a change in the target aspect geometry – all commonly observed in target tracking applications, as discussed.

In the simulation, the non-adaptive tracker uses a detection probability fixed at 0.9 for both the sensors. It is easy to verify from Figure 2(a) that after 30 scans the non-adaptive tracker fails to maintain hold of the target track. The adaptive tracker, instead, is able to also track the abrupt change in the detection probability without losing the target, *i.e.* correctly declaring that the target is present.

In the two examples presented here one way to evaluate the overall detection performance of the trackers is using the time-on-target (ToT) metric, see *e.g.* [5]. Another option, not presented here, would be to compute the OSPA metric [25]. The ToT for the adaptive tracker is 100%, whereas for the non-adaptive is 60% and 63% for the HFSW radar dataset and the simulated dataset, respectively.

5. CONCLUSIONS

This paper presented a target tracking procedure, developed for a network of sensors, which is able to adapt and react to the time-varying changes of the sensors target detection capability. The proposed tracking strategy is based on a Bayesian framework, and the implementation of the tracker is based on the particle filtering approach for the RFS, however, the dynamic target state is augmented with the addition of sensor detection probabilities.

The method was validated using computer simulations and real-world experiments, conducted by the NATO Science and Technology Organization (STO) - Centre for Maritime Research and Experimentation (CMRE). At the cost of some computational complexity in the particle update, with no additional cost in number of particles, it was shown that the ToT metric was greatly improved over the non-adaptive tracking approach. This shows a significant benefit in the use of the adaptive tracker achieving a ToT of 100% vice roughly 60% for the non-adaptive tracker.

6. ACKNOWLEDGEMENTS

This work has been funded by the NATO Allied Command Transformation (NATO-ACT) under the project Maritime Situational Awareness.

7. REFERENCES

[1] Y. Bar-Shalom, P. Willett, and X. Tian, *Tracking and Data Fusion: A Handbook of Algorithms*, YBS Publishing, Storrs, CT, 2011.

[2] E. Mazor, A. Averbuch, , Y. Barshalom, and J. Dayan, “Interacting multiple model methods in target tracking: A survey,” *IEEE Trans. Aerosp. Electron. Syst.*, vol. 34, no. 1, pp. 103–123, Jan. 1998.

[3] M. Basseville and I. V. Nikiforov, *Detection of Abrupt Changes: Theory and Application*, Prentice-Hall, Englewood Cliffs, N.J, 1993.

[4] D. Clark, B. Ristic, Ba-Ngu Vo, and Ba-Tuong Vo, “Bayesian multi-object filtering with amplitude feature likelihood for unknown object SNR,” *IEEE Trans. Signal Process.*, vol. 58, no. 1, pp. 26–37, Jan. 2010.

[5] S. Maresca, P. Braca, J. Horstmann, and R. Grasso, “Maritime surveillance using multiple high-frequency surface-wave radars,” *IEEE Trans. Geosci. Remote Sens.*, vol. 52, no. 8, pp. 5056–5071, Aug. 2014.

[6] P. Braca, P. Willett, K. LePage, S. Marano, and V. Matta, “Bayesian tracking in underwater wireless sensor networks with port-starboard ambiguity,” *IEEE Trans. Signal Process.*, vol. 62, no. 7, pp. 1864–1878, Apr. 2014.

[7] W. Blanding, P. Willett, Y. Bar-Shalom, and S. Coraluppi, “Multisensor track management for targets with fluctuating SNR,” *IEEE Trans. Aerosp. Electron. Syst.*, vol. 45, no. 4, pp. 1275–1292, Oct. 2009.

[8] S. Coraluppi and D. Grimmett, “Multistatic sonar tracking,” in *Proc. of SPIE Conference on Signal Processing, Sensor Fusion, and Target Recognition XII*, Orlando FL, USA, Apr. 2003.

[9] R. Mahler, “Multitarget Bayes filtering via first-order multitarget moments,” *IEEE Trans. Aerosp. Electron. Syst.*, vol. 39, no. 4, pp. 1152–1178, Jan. 2003.

[10] C. Kreucher, A.O. Hero, and K. Kastella, “A comparison of task driven and information driven sensor management for target tracking,” in *44th IEEE Conf. on Decision and Control, 2005 and 2005 European Control Conference (CDC-ECC)*, 2005.

[11] M. R. Morelande, C. M. Kreucher, and K. Kastella, “A Bayesian approach to multiple target detection and tracking,” *IEEE Trans. Signal Process.*, vol. 55, no. 5, pp. 1589–1604, May 2007.

[12] Ba-Tuong Vo, Ba-Ngu Vo, and A. Cantoni, “Bayesian filtering with random finite set observations,” *IEEE Trans. Signal Process.*, vol. 56, no. 4, pp. 1313–1326, Apr. 2008.

[13] O. Erdinc, P. Willett, and Y. Bar-Shalom, “The bin-occupancy filter and its connection to the PHD filters,” *IEEE Trans. Signal Process.*, vol. 57, no. 11, pp. 4232–4246, Nov. 2009.

[14] P. Braca, M. Guerriero, S. Marano, V. Matta, and P. Willett, “Selective measurement transmission in distributed estimation with data association,” *IEEE Trans. Signal Process.*, vol. 58, no. 8, pp. 4311–4321, Aug. 2010.

[15] P. Braca, S. Marano, V. Matta, and P. Willett, “Multitarget-multisensor ML and PHD: Some asymptotics,” in *Proc. of the* 15^{th} *Intern. Conf. on Inform. Fusion (FUSION)*, Singapore, 2012.

[16] P. Braca, S. Marano, V. Matta, and P. Willett, “Asymptotic efficiency of the PHD in multitarget/multisensor estimation,” *IEEE J. Sel. Topics Signal Process.*, vol. 7, no. 3, pp. 553–564, June 2013.

[17] P. Braca, S. Marano, V. Matta, and P. Willett, “A linear complexity particle approach to the exact multi-sensor PHD,” in *in Proc. IEEE Int. Conf. Acoust., Speech, Signal Process. (ICASSP)*, May 2013.

[18] P. Braca, R. Goldhahn, K. LePage, P. Willett, S. Marano, and V. Matta, “Cognitive multistatic auv networks,” in *Proc. of the* 17^{th} *Intern. Conf. on Inform. Fusion (FUSION)*, Salamanca, 2014.

[19] R. Mahler, Ba-Tuong Vo, and Ba-Ngu Vo, “CPHD filtering with unknown clutter rate and detection profile,” *Signal Processing, IEEE Transactions on*, vol. 59, no. 8, pp. 3497–3513, Aug. 2011.

[20] Ba-Tuong Vo, Ba-Ngu Vo, R. Hoseinnezhad, and R. Mahler, “Robust multi-bernoulli filtering,” *IEEE J. Sel. Topics Signal Process.*, vol. 7, no. 3, pp. 399–409, June 2013.

[21] B. Ristic, D. Clark, Ba-Ngu Vo, and Ba-Tuong Vo, “Adaptive target birth intensity for PHD and CPHD filters,” *IEEE Trans. Aerosp. Electron. Syst.*, vol. 48, no. 2, pp. 1656–1668, Apr. 2012.

[22] B. Ristic, Ba-Tuong Vo, Ba-Ngu Vo, and A. Farina, “A tutorial on Bernoulli filters: Theory, implementation and applications,” *IEEE Trans. Signal Process.*, vol. 61, no. 13, pp. 3406–3430, July 2013.

[23] M.S. Arulampalam, S. Maskell, N. Gordon, and T. Clapp, “A tutorial on particle filters for online nonlinear/non-Gaussian Bayesian tracking,” *IEEE Trans. Signal Process.*, vol. 50, no. 2, pp. 174 –188, Feb. 2002.

[24] B.-N. Vo, S. Singh, and A. Doucet, “Sequential Monte Carlo methods for multitarget filtering with random finite sets,” *IEEE Trans. Aerosp. Electron. Syst.*, vol. 41, no. 4, pp. 1224–1245, Oct. 2005.

[25] D. Schuhmacher, B.-T. Vo, and B.-N. Vo, “A consistent metric for performance evaluation of multi-object filters,” *IEEE Trans. Signal Process.*, vol. 56, no. 8, pp. 3447–3457, Aug. 2008.